Liquid Crystals
Publication details, including instructions for authors and subscription information:
http://www.informaworld.com/smpp/title~content=t713926090

Bifurcation and domain walls in thin films of liquid crystals

P. Schiller[a]; G. Pelzl[a]; D. Demus[a]
[a] Sektion Chemie der Martin-Luther-Universität Halle-Wittenberg, Halle (S.), G.D.R.

To cite this Article Schiller, P. , Pelzl, G. and Demus, D.(1989) 'Bifurcation and domain walls in thin films of liquid crystals', Liquid Crystals, 6: 4, 417 — 433
To link to this Article: DOI: 10.1080/02678298908034187
URL: http://dx.doi.org/10.1080/02678298908034187

LIQUID CRYSTALS, 1989, VOL. 6, NO. 4, 417–433

Bifurcation and domain walls in thin films of liquid crystals

by P. SCHILLER, G. PELZL and D. DEMUS
Sektion Chemie der Martin-Luther-Universität Halle-Wittenberg,
WB Physikalische Chemie, DDR-4020 Halle (S.), Mühlpforte 1, G.D.R.

(*Received 14 November 1988; accepted 6 May 1989*)

A perturbation method is proposed to determine the bifurcation diagram for instabilities in thin liquid-crystalline layers which are subject to an external magnetic or electric field. Different types of continuous and discontinuous field-induced director reorientations can be classified by using elementary bifurcation theory. When two differently oriented director positions are stable, domains may appear. For weakly distorted samples the structure and velocity of walls between stable differently oriented domains is described by a solitary wavy solution of the non-linear director equation. The results of the perturbation method are applied to nematic and smectic C films.

1. Introduction

The investigation of field-induced instabilities in liquid-crystalline layers provides a simple means to determine the material parameters [1]. Furthermore, various applications of director reorientations are possible. The switching characteristics can be varied appropriately by optimizing the geometrical conditions and the values of the elastic constants. In such a way continuous and discontinuous transitions result. When the initial director position becomes unstable after applying the field, the director switches simultaneously towards a stable state over the entire sample. However, if the initial position is metastable, transitions proceed by domain wall motion. The aim of this paper is the investigation of domain walls which appear in weakly distorted layers close to bifurcation points. This problem implies the determination of the bifurcation diagrams for field induced transitions. For simplicity we restrict our attention to plane walls, but it should be mentioned that an extension of the perturbation method to weakly curved walls is also possible.

Figure 1 shows a domain wall in a nematic liquid crystal subjected to a magnetic field. If the field strength exceeds a definite value, two stable director configurations are possible. For a somewhat inclined direction of the magnetic field, walls between differently oriented domains move through the sample in such a way, that absolutely stable domains grow at the cost of metastable domains. When the magnetic field is perpendicular to the plates, both domain types are equally stable and the wall velcoity vanishes. For this geometry Brochard [2] determined the wall structure theoretically. He also estimated the velocity of the moving walls in tilted magnetic fields by comparing the entropy production with the released field energy. To describe travelling walls Wang [3] introduced a simplified mathematical approach using certain unproved assumptions. Lin and Shu [4] commented on some results in Wang's paper and compared them with the experimental results obtained by Leger [5].

As a second example we consider a smectic C phase in an external electric field (see figure 2). The director in a smectic C liquid crystal is confined on the surface of a cone

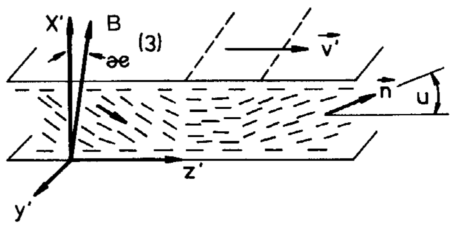

Figure 1. Domain wall in a planar nematic layer subject to a tilted magnetic field. Here B is the magnetic flux density, $\kappa^{(3)}$ is the tilt angle of B, v' is the wall velocity, u is the director rotation angle and x', y' z' are cartesian coordinates.

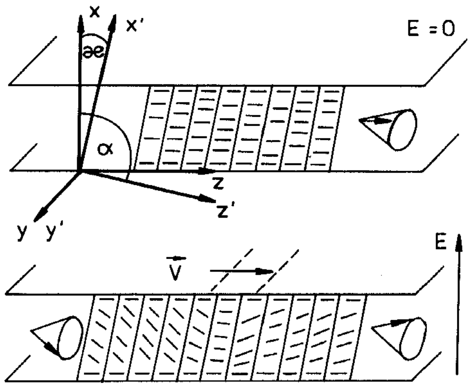

Figure 2. Domain wall in a S_C film. E is the electric field, κ is the tilt of the smectic layers with respect to the sample surfaces, α is the angle between the normal of the smectic layers and the direction of the electric field and v is the velocity of the domain wall. x', y', z' and x, y, z, are cartesian coordinates.

with an aperture 2θ. After applying the field domains may appear, which differ in the rotation direction. In contrast to the previous example it is not necessary to tilt the field to obtain moving walls. Already if the smectic layers are not exactly perpendicular to the boundary plates, domains with differently aligned directors are no longer equally stable and wall motion is generated. Some theoretical results in [6] are related to the case of large fields which significantly exceed the Freedericks threshold. In §5.2. we consider solitary waves in S_C films at fields close to the Freedericks threshold. It should be noted, that solitary waves generated mechanically can be regarded as fast moving walls. In this topic many interesting results have been found for nematic liquid crystals [7, 8]. An insight into the mathematical treatment is given in [9, 10].

2. Bifurcating solutions of the director equation

Consider a liquid-crystalline layer between plates at $X = 0$ and $X = d$. Excluding pattern formation we assume that a distorted state of the sample is described by a scalar function $u(X)$, which is usually the rotation angle of the director, u is equal to zero for the homogeneously aligned initial state at the vanishing field strength. For convenience dimensionless coordinates

$$x = \frac{\pi X}{d}$$

are introduced, so that the thin layer is located within the interval

$$0 \leqslant x \leqslant \pi.$$

The free energy of the liquid-crystalline layer is the functional

$$F[u] = \frac{1}{2}\int_0^\pi dx\,[g(u)u_x^2 + f(u)], \tag{1}$$

where

$$u_x = \frac{\partial u}{\partial x}.$$

As the director is fixed at the boundaries, the conditions

$$u(0) = 0 \quad \text{and} \quad u(\pi) = 0 \tag{2}$$

have to be satisfied.

When backflow effects are neglected, the dynamics of the director is described by the equation of motion

$$u_\tau = -\frac{\delta F}{\delta u}, \tag{3}$$

where τ is proportional to the time. For an equilibrium state the torque balance equation (3) reduces to the Euler–Lagrange equation

$$u_{xx}g(u) + \tfrac{1}{2}g'(u)u_x^2 - \tfrac{1}{2}f'(u) = 0. \tag{4}$$

The analytic functions f and g are expanded in series

$$\left.\begin{aligned} g(u) &= 1 + g_2u + g_3u^2 + \ldots, \\ f(u) &= f_0u + f_1u^2 + f_2u^3 + f_3u^4 + \ldots. \end{aligned}\right\} \tag{5}$$

We note that the special choice $g_1 = 1$ involves a suitable definition of the dimensionless time in equation (3). Insertion of the series (5) in equation (4) leads to

$$-\tfrac{1}{2}f_0 + (u_{xx} - f_1u) + (g_2uu_{xx} + \tfrac{1}{2}g_2u_x^2 - \tfrac{3}{2}f_2u^2) + (g_3u^2u_{xx} + g_3uu_x^2 - 2f_3u^3) + \ldots = 0. \tag{6}$$

In this case the homogeneous director alignment, $u = 0$, is compatible with equation (6), only when

$$f_0 = 0. \tag{7}$$

Now we investigate, how non-trivial solutions of equation (6) emerge from the initial state $u = 0$ at a bifurcation point. Such a point is found by solving (6) in the linear approximation,

$$u_{xx} - f_1u = 0. \tag{8}$$

This equation and the boundary conditions in equation (2) define a linear eigenvalue problem. The eigenvalue with the smallest value $|f_1|$ is physical relevant. This eigenvalue is $f_1 = -1$ with the corresponding eigenfunction

$$u = a\sin x. \tag{9}$$

The relation

$$f_1 = -(1 + \mu) \tag{10}$$

ntroduces a bifurcation parameter μ, which is assumed to be small in our calculations $|\mu| \ll 1$). Furthermore, we define a norm for functions $u(x)$ by

$$\varepsilon = \max_{0 \leqslant x \leqslant \pi} |u(x)| \tag{11}$$

Close to the bifurcation point $\mu = 0$ the norm of branching solutions of equation (6) is also a small quantity ($\varepsilon \ll 1$). ε characterizes the order of magnitude for any quantities defined in the framework of the perturbation treatment. Equation (6) is solved stepwise using the expansions

$$\left.\begin{aligned} u &= u^{(1)} + u^{(2)} + u^{(3)} + \dots, \\ \mu &= \mu^{(1)} + \mu^{(2)} + \dots, \end{aligned}\right\} \tag{12}$$

where the superscript defines the order of magnitude

$$u^{(1)} \sim \varepsilon, \quad u^{(2)} \sim \varepsilon^2, \quad u^{(3)} \sim \varepsilon^3, \dots$$

and

$$\mu^{(1)} \sim \varepsilon, \quad \mu^{(2)} \sim \varepsilon^2, \dots .$$

Insertion of expansions (12) and collection of all terms with the same order of magnitude leads to a hierarchy of differential equations

$$\left.\begin{aligned} u_{xx}^{(1)} + u^{(1)} &= 0, \\ u_{xx}^{(2)} + u^{(2)} &= L^{(2)}, \\ u_{xx}^{(3)} + u^{(3)} &= L^{(3)}, \end{aligned}\right\} \tag{13}$$

with

$$L^{(2)} = -\mu^{(1)}u^{(1)} - g_2[u_{xx}^{(1)}u^{(1)} + \tfrac{1}{2}(u_x^{(1)})^2] + \tfrac{3}{2}f_2(u^{(1)})^2,$$

and

$$\begin{aligned} L^{(3)} = & -\mu^{(1)}u^{(2)} - \mu^{(2)}u^{(1)} - g_2[u_{xx}^{(1)}u^{(2)} + u_{xx}^{(2)}u^{(1)} + u_x^{(1)}u_x^{(2)}] \\ & + 3f_2u^{(1)}u^{(2)} + 2f_3(u^{(1)})^3 - g_3[(u^{(1)})^2u_{xx}^{(1)} + u^{(1)}(u_x^{(1)})^2]. \end{aligned}$$

The first differential equation has the solution

$$u^{(1)} = a \sin x \quad (a \equiv a^{(1)}), \tag{14}$$

where a can be chosen arbitrarily. This solution is inserted into the second equation of the hierarchy (13). Because the eigenvalue problem

$$u_{xx}^{(2)} + u^{(2)} = \lambda u^{(2)}$$

with the boundary conditions of equation (2) has the non-trivial solution

$$u^{(2)} = a^{(2)} \sin x$$

for $\lambda = 0$, the condition of solubility

$$\int_0^\pi dx L^{(2)} \sin x = 0 \tag{15}$$

has to be satisfied (Fredholm's theorem).

The integration yields

$$-\mu^{(1)}a + \left(\frac{2g_2 + 4f_2}{\pi}\right)a^2 = 0. \qquad (16)$$

This equation has the solutions

$$\left.\begin{aligned} a &= 0 \\ \text{and} \qquad \mu^{(1)} &= \left(\frac{2g_2 + 4f_2}{\pi}\right)a \end{aligned}\right\} \qquad (17)$$

which describe the branches of a transcritical bifurcation (see figure 3). Stable states (the solid lines) correspond to a minimum of the free energy (1) and unstable states (dashed lines) to a maximum.

Frequently, symmetry requirements are accompanied with the condition

$$g_2 + 2f_2 = 0. \qquad (18)$$

In these cases

$$\mu^{(1)} = 0 \qquad (19)$$

results and the distortion amplitude is determined by the last equation (13). In analogy to equation (15) Fredholm's theorem leads to

$$\int_0^\pi dx\, L_3 \sin x = 0 \qquad (20)$$

or explicitly

$$-\mu^{(2)}a + (\tfrac{3}{2}f_3 + \tfrac{1}{4}g_3)a^3 = 0. \qquad (21)$$

This equation has two solutions, which describe either a supercritical or a subcritical bifurcation, depending on the sign of $6f_3 + g_3$ (see figure 3).

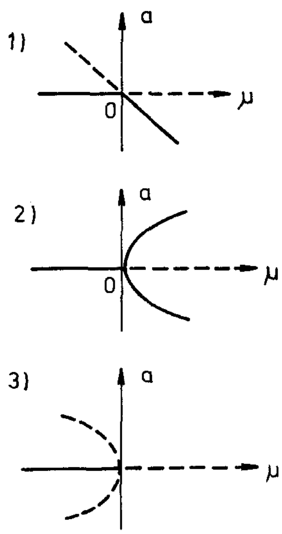

Figure 3. Bifurcation diagrams (μ is the control parameter and a is the distortion amplitude). Solid lines correspond to stable states and dashed lines to unstable states. (1) transcritical bifurcation ($2g_2 + 4f_2 \neq 0$) (2) supercritical bifurcation ($2g_2 + 4f_2 = 0$, $6f_3 + g_3 > 0$) (3) subcritical bifurcation ($2g_2 + 4f_2 = 0$, $6f_3 + g_3 < 0$).

3. Bistability

Rapid convergence of the perturbation expansion requires that distortions are small. This condition necessarily restricts a general investigation of bistable layers with the aid of perturbation methods. In this paper we shall not consider the subcritical bifurcation further, but for the transcritical case the suppositions

$$\left.\begin{aligned} g_2 &= g^{(1)} \quad \text{and} \quad f_2 = f^{(1)}, \\ (g^{(1)} &\sim \varepsilon \quad \text{and} \quad f^{(1)} \sim \varepsilon), \end{aligned}\right\} \tag{22}$$

guarantee that all solutions of the director equation have small distortion amplitudes. Clearly, these relations also involve the supercritical bifurcation with $f_2 = g_2 = 0$. Furthermore, it is possible to include imperfect bifurcations [11] by assuming that $f_0 \neq 0$. For example, an imperfect bifurcation results, when the director is somewhat tilted at the boundaries [12].

If $f_0 \neq 0$, we make the assumption

$$f_0 = f^{(3)},$$

where (23)

$$f^{(3)} \sim \varepsilon^3.$$

Taking into account the relations (22) and (23), the set of equations (12) is replaced by

$$\left.\begin{aligned} u_{xx}^{(1)} + u^{(1)} &= 0, \\ u_{xx}^{(2)} + u^{(2)} &= -\mu^{(1)}u^{(1)}, \\ u_{xx}^{(3)} + u^{(3)} &= -\mu^{(1)}u^{(2)} - \mu^{(2)}u^{(1)} + \tfrac{1}{2}f^{(3)} \\ &\quad - g^{(1)}[u_{xx}^{(1)}u^{(1)} + \tfrac{1}{2}(u_x^{(1)})^2] + \tfrac{3}{2}f^{(1)}(u^{(1)})^2 \\ &\quad - g_3[(u^{(1)})^2u_{xx}^{(1)} + u^{(1)}(u_x^{(1)})^2] \\ &\quad + 2f_3(u^{(1)})^3. \end{aligned}\right\} \tag{24}$$

The solution of the first equations is

$$u^{(1)} = a\sin x. \tag{25}$$

Inserting this solution in the right hand side of the equation for $u^{(2)}$ and applying Fredholm's theorem (15) we obtain

$$\mu^{(1)} = 0. \tag{26}$$

Finally, the solubility condition for the last equation of the set (24) yields

$$a^3 + \beta^{(1)}a^2 + \beta_a^{(2)} + \beta^{(3)} = 0, \tag{27}$$

where

$$\left.\begin{aligned} \beta &= \tfrac{1}{4}(6f_3 + g_3), \quad \beta^{(1)} = \frac{1}{\beta}\left(\frac{2}{\pi}\right)(g^{(1)} + 2f^{(1)}), \\ \beta^{(2)} &= -\frac{\mu^{(2)}}{\beta} \quad \text{and} \quad \beta^{(3)} = \frac{1}{\beta}\left(\frac{2}{\pi}\right)f^{(3)}. \end{aligned}\right\} \tag{28}$$

Equation (27) has either one or three real solutions. In the latter case two solutions correspond to stable states and the third to an unstable stationary state. The

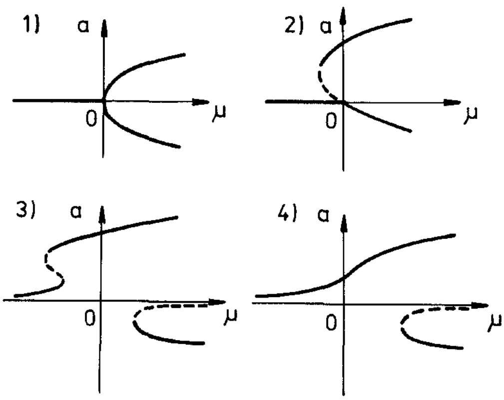

Figure 4. Bifurcation diagrams corresponding to equation (27). Solid lines are assigned to stable states and dashed lines to unstable states. The coefficients in equation (27) are chosen differently ($\mu = \mu^{(2)}$ is a control parameter and a is the distortion amplitude): (1) $\beta > 0$, $\beta^{(1)} = \beta^{(3)} = 0$; (2) $\beta > 0$, $\beta^{(1)} \neq 0$, $\beta^{(3)} = 0$; (3) $\beta > 0$, $\beta^{(3)} \neq 0$, $27(\beta^{(3)})^2 < (\beta^{(1)})^3\beta^{(3)}$; (4) $\beta > 0$, $\beta^{(3)} \neq 0$, $27(\beta^{(3)})^2 > (\beta^{(1)})^3\beta^{(3)}$.

bifurcation diagrams are obtained by plotting a versus $\mu^{(2)}$; for $\beta > 0$ such diagrams are shown in figure 4. When $\beta^{(3)} \neq 0$, then there is not a bifurcation point and two separate solution branches appear (imperfect bifurcation).

4. Domain walls

Transitions from a metastable to an absolutely stable state proceed by travelling domain walls. Let us assume, that the z axis of a cartesian system is parallel to the plates and perpendicular to the normal of a plane wall (see figure 1). Generalizing the free energy (1) to the two dimensional case we obtain

$$F[u] = \frac{1}{2}\int dz \int_0^{\pi} dx\, [g(u)u_x^2 + h(u)u_z^2 + m(u)u_x u_z + f(u)] \tag{29}$$

and the corresponding boundary conditions for u are

$$\left.\begin{aligned} u(x = 0, z, \tau) &= u(x = \pi, z, \tau) = 0, \\ \lim_{z\to\infty} u_z(x, z, \tau) &= \lim_{z\to-\infty} u_z(x, z, \tau) = 0. \end{aligned}\right\} \tag{30}$$

The boundary conditions imply that far away from the domain wall the director alignment does not depend on the coordinate z. Now the equation of motion (3) takes the form

$$\begin{aligned} &u_{xx}g(u) + \tfrac{1}{2}g'(u)u_x^2 + u_{zz}h(u) + \tfrac{1}{2}h'(u)u_z^2 \\ &+ m(u)u_{xz} + \tfrac{1}{2}m'(u)u_x u_z - \tfrac{1}{2}f'(u) = u_\tau . \end{aligned} \tag{31}$$

The non-linear functions f, g, h, and m are expanded in the series

$$\left.\begin{aligned} g(u) &= 1 + g^{(1)}u + g_3u^2 + \dots, \\ f(u) &= f^{(3)}u - (1 + \mu)u^2 + f^{(1)}u^3 + f_3u^4 + \dots, \\ h(u) &= h_1 + h_2u + h_3u^2 + \dots, \\ m(u) &= m^{(1)} + m_2u + m_3u^2 + \dots, \end{aligned}\right\} \tag{32}$$

Besides the assumptions (22) and (23) for obtaining weakly distorted director configurations the additional requirement $|m_1| = |m^{(1)}| \ll 1$ should be satisfied. This condition is strictly valid for nematic layers, because in these cases $m_1 = 0$. We seek solitary wave solutions of equation (31) to describe walls, which travel with a constant velocity v. The Galilei transformation

$$\xi = z - v\tau \tag{33}$$

reduces the number of variables. Thus we have

$$u = u(x, \xi), \quad u_z = u_\xi \quad \text{and} \quad u_\tau = vu_\xi .$$

The perturbation calculation starts with the expansions

$$\left.\begin{aligned} u &= u^{(1)} + u^{(2)} + u^{(3)} + \dots, \\ \mu &= u^{(1)} + u^{(2)} + \dots, \\ v &= v^{(1)} + v^{(2)} + \dots, \\ \varrho &= \xi(\omega^{(1)} + \omega^{(2)} + \dots). \end{aligned}\right\} \tag{34}$$

and

The scaling of the coordinate ξ in the last expansion takes into consideration that the domain wall width diverges when the bifurcation point ($\mu = 0$ in the case of a supercritical bifurcation) is approached [5]. The expansion parameters $\omega^{(n)}$ are determined by non-linear boundary value problem, which result from the perturbation theory. To the lowest order of magnitude the derivatives of u are found to be

$$\left.\begin{aligned} u_{\xi\xi} &= (\omega^{(1)})^2 u^{(1)}_{\varrho\varrho} + O(\varepsilon^4), \\ vu_\xi &= v^{(1)}\omega^{(1)}u^{(1)}_\varrho + O(\varepsilon^4), \\ u_{x\xi} &= \omega^{(1)}u^{(1)}_x + O(\varepsilon^3). \end{aligned}\right\} \tag{35}$$

Inserting expansions (34) and (35) into equation (31) and arranging all terms according to their order of magnitude, the system of equations

$$\left.\begin{aligned} u^{(1)}_{xx} + u^{(1)} &= 0, \\ u^{(2)}_{xx} + u^{(2)} &= R^{(2)}, \\ u^{(3)}_{xx} + u^{(3)} &= R^{(3)} \end{aligned}\right\} \tag{36}$$

results with the abbreviations

$$\begin{aligned} R^{(2)} &= -\mu^{(1)}u^{(1)}, \\ R^{(3)} &= -\mu^{(1)}u^{(2)} - \mu^{(2)}u^{(1)} - g^{(1)}u^{(1)}u^{(1)}_{xx} - \tfrac{1}{2}g^{(1)}(u^{(1)}_x)^2 - h_1(\omega^{(1)})^2u^{(1)}_{\varrho\varrho} \\ &\quad - m^{(1)}\omega^{(1)}u^{(1)}_{x\varrho} - m_2u^{(1)}\omega^{(1)}u^{(1)}_{x\varrho} - \tfrac{1}{2}m_2u^{(1)}_x\omega^{(1)}u^{(1)}_\varrho + \tfrac{1}{2}f^{(3)} \\ &\quad + \tfrac{3}{2}f^{(1)}(u^{(1)})^2 + 2f_3(u^{(1)})^3 + v^{(1)}\omega^{(1)}u^{(1)}_\varrho - g_3u^{(1)}(u^{(1)}_x)^2 \\ &\quad - g_3u^{(1)}_{xx}(u^{(1)})^2 . \end{aligned}$$

The first equation of the system (36) has the solution

$$u^{(1)} = a(\varrho)\sin x \tag{37}$$

with $a(\varrho) \equiv a^{(1)}(\varrho)$. The solubility condition for the second equation of the system (36) leads to

$$\int_0^\pi R^{(2)} \sin x \, dx = -\tfrac{1}{2}\pi\mu^{(1)}a^{(1)} = 0, \tag{38}$$

so that for any non-trivial solution ($a \neq 0$)

$$\mu^{(1)} = 0. \tag{39}$$

Because $R^{(2)} = 0$, the second equation of the system (36) is solved by

$$u^{(2)} = a^{(2)}(\varrho) \sin x. \tag{40}$$

Finally, the condition of solubility

$$\int_0^\pi R^{(3)} \sin x \, dx = 0 \tag{41}$$

is applied to obtain the function $a(\varrho)$. Taking into account the results (37), (39) and (40), a non linear differential equation is derived from equation (41)

$$h_1(\omega^{(1)})^2 a_{\varrho\varrho} - v^{(1)}\omega^{(1)} a_\varrho = \beta(a^3 + \beta^{(1)}a^2 + \beta^{(2)}a + \beta^{(3)}). \tag{42}$$

The polynomial on the right hand side of equation (42) has three real roots

$$a_A \leqslant a_B \leqslant a_C, \tag{43}$$

when the director alignment is bistable. Then we have

$$h_1 a_{\xi\xi} - v^{(1)} a_\xi = \beta(a - a_A)(a - a_B)(a - a_C), \tag{44}$$

where the coordinate ϱ is replaced by ξ according to the transformation (35). Equation (44) with boundary conditions

$$\lim_{\xi \to \infty} a_\xi = \lim_{\xi \to -\infty} a_\xi = 0 \tag{45}$$

has the solution [13]

$$a(\xi) = a_A + \frac{a_C - a_A}{1 + \exp(w^{(1)}\xi)}, \tag{46}$$

where

$$w^{(1)} = (a_C - a_A)\sqrt{\left(\frac{\beta}{2h_1}\right)} \tag{47}$$

and

$$v^{(1)} = (a_A + a_C - 2a_B)\sqrt{\left(\frac{\beta}{2h_1}\right)}. \tag{48}$$

Thus the solitary wave solution is determined by

$$u(x, z - v\tau) = \left(a_A + \frac{a_C - a_A}{1 + \exp w(z - v\tau)}\right)\sin x + O(\varepsilon^2), \tag{49}$$

where we have omitted the superscripts of $v^{(1)}$ and $w^{(1)}$. This result describes a travelling domain wall, which separates two domains with distortion amplitudes a_A and a_C.

5. Examples of bistable layers

5.1. *Planar nematic layer in a magnetic field*

We restrict our attention to the special geometry illustrated in figure 1. The tilt of the magnetic field is assumed to be small ($|\kappa^{(3)}| \ll 1$), so that two weakly distorted director configurations are stable at moderate magnetic fields. Applying the continuum theory of nematic liquid crystals [1], the free energy is expressed as the functional

$$f = \int dz' \int dx' \,(f_A + f_B), \tag{50}$$

where

$$\begin{aligned} f_A &= \tfrac{1}{2}(K_{11}\cos^2 u + K_{33}\sin^2 u)\left(\frac{\partial u}{\partial x'}\right)^2 + \tfrac{1}{2}(K_{11}\sin^2 u + K_{33}\cos^2 u)\left(\frac{\partial u}{\partial z'}\right)^2 \\ &\quad + (K_{33} - K_{11})\sin u \cos u\left(\frac{\partial u}{\partial x'}\right)\left(\frac{\partial u}{\partial z'}\right) \\ f_B &= -\tfrac{1}{2}\Delta\chi B^2 \sin^2(u + \kappa^{(3)}), \end{aligned} \tag{51}$$

K_{11}, K_{22} and K_{33} are the elastic constants of the Frank–Oseen–theory, $\Delta\chi$ denotes the anisotropy of the magnetic susceptibility, B is the magnetic flux density and the $x'y'$ coordinate system is defined in figure 1. The director angle u obeys the equation of motion

$$-\frac{\delta f}{\delta u} = \lambda \frac{\partial u}{\partial t}, \tag{52}$$

where t is the time, and λ is the rotational viscosity. With the transformations

$$x = \frac{\pi}{d}x', \quad z = \frac{\pi}{d}z' \quad \text{and} \quad \tau = \frac{\pi^2 K_{11} t}{d^2 \lambda}, \tag{53}$$

dimensionless coordinates and a dimensionless time are introduced, and the integrand of the integral (50) is expanded in powers of u. The result is the functional

$$\begin{aligned} F = \frac{1}{2}\int dz \int_0^{\pi} dx \Bigg[& u_x^2 + k u_x^2 u^2 + r u_z^2 - k u_z^2 u^2 + k u\, u_x u_z \\ & - u^2\left(1 + \frac{B^2 - B_0^2}{B_0^2}\right) + \frac{B^2}{B_0^2}\left(\frac{u^4}{3} - 2\kappa^{(3)} u\right)\Bigg], \end{aligned} \tag{54}$$

where

and

$$\left.\begin{aligned} F &= \frac{f}{K_{11}} + O(\varepsilon^6), \\ k &= \frac{K_{33} - K_{11}}{K_{11}}, \quad r = \frac{K_{33}}{K_{11}}, \quad B_0 = \frac{\pi}{d}\sqrt{\left(\frac{K_{11}}{\Delta\chi}\right)}. \end{aligned}\right\} \tag{55}$$

Comparing the functionals (29) and (54), we identify the coefficients in the expansions (32) as

$$\left.\begin{aligned} g^{(1)} &= 0, \quad g_3 = k, \\ f^{(1)} &= 0, \quad f_1 = -1 - \frac{B^2 - B_0^2}{B_0^2}, \\ f_3 &= \frac{B^2}{3B_0^2}, \quad f^{(3)} = -\frac{2B^2\kappa^{(3)}}{B_0^2}, \\ h_1 &= r \quad \text{and} \quad m^{(1)} = 0. \end{aligned}\right\} \tag{56}$$

Combining the relations (56) and (28) yields

$$\left.\begin{aligned} \beta &= \frac{B^2}{2B_0^2} + \frac{k}{4}, \quad \beta^{(1)} = 0 \\ \beta^{(2)} &= \frac{B^2 - B_0^2}{B_0^2\beta} \quad \text{and} \quad \beta^{(3)} = -\frac{4B^2\kappa^{(3)}}{\pi B_0^2\beta} \end{aligned}\right\} \tag{57}$$

and equation (27) is determined explicitly by

$$a^3 - \left(\frac{B^2 - B_0^2}{B_0^2\beta}\right)a - \left(\frac{4B^2}{\pi B_0^2\beta}\right)\kappa^{(3)} = 0. \tag{58}$$

According to this equation the bifurcation is either supercritical for $\kappa^{(3)} = 0$ or imperfect, when the magnetic field is somewhat tilted to the plate normal. The latter case is illustrated in the bifurcation diagram given in figure 5. The arrow indicates the transition from a metastable to an absolutely stable director configuration by wall motion. With the roots a_A, a_B and a_C of equation (58) the structure and velocity of a domain wall is determined by equations (49), (47) and (48).

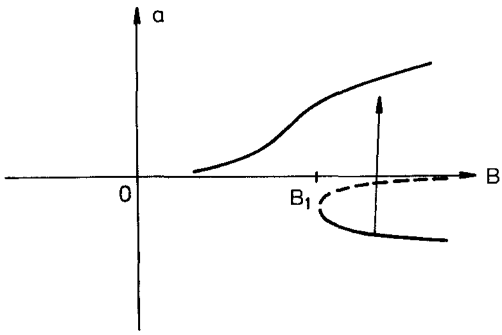

Figure 5. Bifurcation diagram of a nematic layer in an inclined magnetic field. B is the magnetic flux density and a is the distortion amplitude. The arrow indicates the transition from the metastable to the absolutely stable director configuration.

For a qualitative discussion let us assume that $K_{11} = K_{33}$ ($k = 0$). Then equation (58) reduces to

$$a^3 - 2\left(\frac{B^2 - B_0^2}{B^2}\right)a - \frac{8}{\pi}\kappa^{(3)} = 0 \tag{59}$$

and the limit of bistability B_l (see figure 5) is found to be

$$B_l = \left[1 + \frac{3}{4}\sqrt[3]{\left\{\frac{4}{\pi}(\kappa^{(3)})^2\right\}}\right] B_0. \tag{60}$$

It can be checked easily, that the domain wall velocity has a maximum value for $B = B_l$. Using formula (48) for v and taking into account the transformations (53), this velocity can be expressed in conventional units as

$$v'(B_l) = \frac{3\pi B_l \sqrt[3]{\left(\frac{4}{\pi}\kappa^{(3)}\right)} K_{11}}{2\lambda d B_0}. \tag{61}$$

5.2. *Planar oriented smectic C film in an electric field*

The director position in smectic C phases is uniquely determined by an azimuthal angle Φ, as the director is confined to the surface of a cone (see figure 6). Let us consider a domain wall in a planar oriented sample; this geometry is presented in figure 2. In [6] the free energy

$$f = \frac{1}{2}\int dz' \int dx' \left[B_{\parallel}\left(\frac{\partial \Phi}{\partial x'}\right)^2 + B_{\perp}\left(\frac{\partial \Phi}{\partial z'}\right)^2 - \Delta\varepsilon E^2 (\cos\alpha\cos\theta + \sin\theta\sin\alpha\cos\Phi)^2\right], \tag{62}$$

is derived, where $B_{\parallel}$ and $B_{\perp}$ are elastic constants, α, is the angle between the field direction and the layer normal, $\Delta\varepsilon$ is the dielectric anisotropy ($\Delta\varepsilon > 0$) and E is the electric field strength. By simple geometrical considerations the relations

$$\left.\begin{aligned} \kappa &= \alpha - \frac{\pi}{2} \\ \text{and} \qquad \cos\Phi_0 &= \frac{\tan\kappa}{\tan\theta} \end{aligned}\right\} \tag{63}$$

are obtained, where κ is the layer tilt angle (see figure 2) and Φ_0 corresponds to the director position of the undistorted sample. Any distortions in the sample are determined by

$$u = \Phi - \Phi_0 \tag{64}$$

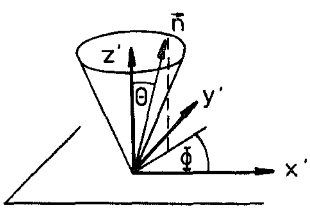

Figure 6. Director rotation in the S_C phase. **n** is the director, Φ is the azimuthal angle of the director, and θ is the tilt angle of the director with respect to the normal of the smectic layer plane. x', y' and z' are cartesian coordinates.

and the evolution of u is governed by

$$\frac{\delta f}{\delta u} = -\lambda \frac{\partial u}{\partial t} \tag{65}$$

in complete analogy to equation (52). The transformations

$$\left.\begin{aligned} \tau &= \frac{\pi^2(B_{\parallel}\cos^2\kappa + B_{\perp}\sin^2\kappa)}{d^2\lambda}\, t, \\ x &= \frac{\pi}{d}(x'\cos\kappa - z'\sin\kappa), \\ z &= \frac{\pi}{d}(x'\sin\kappa + z'\cos\kappa) \end{aligned}\right\} \tag{66}$$

define a dimensionless time τ and a coordinate system, which is fixed at the bounding plates of the sample (see figure 2). Then the free energy (62) is rewritten as

$$F = \frac{1}{2}\int dz \int_0^{\pi} dx \left[u_x^2 + h_1 u_z^2 + m_1 u_x u_z - \frac{\Delta\varepsilon E^2 \sin^2\theta \cos^2\kappa d^2}{B_{\rm el}\pi^2} (\cos(\Phi_0 + u) - \cos\Phi_0)^2 \right], \tag{67}$$

where

$$\begin{aligned} F &= \frac{f}{B_{\rm el}}, \\ B_{\rm el} &= B_{\parallel}\cos^2\kappa + B_{\perp}\sin^2\kappa, \\ h_1 &= \frac{1}{B_{\rm el}}(B_{\parallel}\sin^2\kappa + B_{\perp}\cos^2\kappa) \end{aligned} \tag{68}$$

and

$$m_1 = \frac{2}{B_{\rm el}}(B_{\parallel} - B_{\perp})\cos\kappa\sin\kappa.$$

Substituting f and t by F and τ, respectively the equation of motion (64) is converted to the dimensionless form (31). The integrand of F is expanded

$$F = \frac{1}{2}\int dz \int_0^{\pi} dx\, [u_x^2 + h_1 u_z^2 + m_1 u_x u_z + f_1 u^2 + f_2 u^3 + f_3 u^4 + \ldots], \tag{69}$$

with

$$\left.\begin{aligned} f_1 &= -1 - \frac{E^2 - E_0^2}{E^2}, \quad f_2 = \frac{\tan\kappa}{\tan\theta}, \\ f_3 &= \frac{E^2}{3E_0^2}, \\ E_0 &= \frac{\pi}{d\sin\theta\cos\kappa\sin\Phi_0}\sqrt{\left(\frac{B_{\rm el}}{\Delta\varepsilon}\right)}. \end{aligned}\right\} \tag{70}$$

The conditions (22) for obtaining weakly distorted director configurations turn out to be satisfied, when the layer tilt κ is small compared to θ

$$\kappa \equiv \kappa^{(1)} \ll \theta, \tag{71}$$

so that

$$f_2 = f^{(1)} \quad \text{and} \quad m_1 = m^{(1)}. \tag{72}$$

By comparing the functionals (69) and (29) the coefficients (28) are identified and, inserted in equation (27), give

$$a^3 + \frac{8E_0^2 \tan\kappa}{\pi E^2 \tan\theta} a^2 + 2\frac{E^2 - E_0^2}{E^2} a = 0 \tag{73}$$

For $E > E_1$ with

$$E_1 = E_0\left[1 - \frac{4}{\pi^2}\left(\frac{\tan\kappa}{\tan\theta}\right)^2\right] + O(\varepsilon^4), \tag{74}$$

the system is bistable

Figure 7 shows the bifurcation diagram, which corresponds to equation (73). The arrows indicate possible transitions from a metastable to an absolutely stable state by travelling walls. Let us determine the wall velocity v from equation (48). When the solutions of equation (73) are arranged according to their magnitude ($a_A \leqslant a_B \leqslant a_C$), two cases have to be distinguished.

If $E \geqslant E_0$, we have

and

$$\left.\begin{aligned} a_A &= r - R, \quad a_B = 0 \\ a_C &= r + R, \end{aligned}\right\} \tag{75}$$

where

$$R = \sqrt{\left(r^2 + 2\frac{E^2 - E_0^2}{E^2}\right)}$$

and

$$r = \frac{4\tan\kappa}{\pi\tan\theta}.$$

Expressing the dimensionless velocity (48) in conventional units ($V = \pi B_{\text{el}} d^{-1}\lambda^{-1} v$), we obtain

$$V = \frac{\pi r B_{\text{el}} E}{\lambda d\sqrt{h_1} E_0}. \tag{76}$$

Similarly, for $E_1 \leqslant E \leqslant E_0$ we find

$$a_A = 0, \quad a_B = R - r \quad \text{and} \quad a_C = R + r, \tag{77}$$

so that

$$V = \frac{\pi(3R - r) B_{\text{el}} E}{2\lambda d\sqrt{h_1} E_0}. \tag{78}$$

Obviously, for $E = E_2$ with

$$E_2 = E_0\left[1 - \frac{32}{9\pi^2}\left(\frac{\tan\kappa}{\tan\theta}\right)^2\right] + O(\varepsilon^4) \quad (79)$$

the direction of the velocity is reversed.

Finally, let us remark, that perturbation techniques are also suitable to determine the bifurcation diagram of more complicated systems. In [12] the Freedericksz transition in twisted layers of nematic and cholesteric liquid crystals has been considered. The results of the perturbation expansion for small and moderate distortion angles are well confirmed by numerical calculations.

6. Discussion

The perturbation method used in this paper provides a general procedure for describing field-induced domain walls in weakly distorted liquid crystal layers. In principle, approximations of higher order in terms of the parameter ε can also be obtained in a systematic manner. This problem has been solved for determining bifurcation diagrams of twisted nematic liquid crystals [12]. However, higher order corrections of the domain wall solution (49) are rather complicated. The results of this paper concerning domain wall motion in nematics can be compared with other approaches in the literature.

6.1. *Nematic layer*

Recently, Wang [3] has derived a solitary wave equation by using an ansatz, which is written as

$$u(x, z, t) = \theta_0(x)\theta_1(x, z, t), \quad (80)$$

in our notation. Here $\theta_0(x)$ is a rapidly varying function of x and θ_1 is slowly varying with x (t is the time). Yu-zhang and Zhong-can [14] criticized the rather intuitive mathematical procedure in [3]. In another comment Lin and Shu [4] pointed out, that a condition for the occurrence of walls resulting from Wang's approach contradicts the experimental data obtained by Leger [5]. Nevertheless, Wang has obtained a similar solitary wave equation for the magnitude of θ_1 as derived with the perturbation method in this paper. Therefore let us discuss the experimental results of Leger [5] in comparison to the conclusions drawn from the solitary wave solution (49) which is applied to a nematic layer in an inclined magnetic field.

Leger found that the domain wall velocity, v, decreases with increasing magnetic flux density, B. This behaviour is in accord with equation (48) for v, when the roots a_A, a_B and a_C of equation (59) are inserted. But our procedure for fitting experimental data would be different from that of Leger, who assumed the dependence

$$v \sim \frac{1}{B - B_0}, \quad (81)$$

(B_0 is the Freedericksz threshold for $\kappa^{(3)} = 0$) which was suggested by Brochard [2]. However, the solitary wave solution (49) is only applicable in the bistable region, namely if $B \geqslant B_1$ (see figure 5). Leger has also obtained wall velocities outside the bistable region (for $B < B_1$) as Lin and Shu [4] emphasized. Clearly, outside the bistable region the solutions of the solitary wave equation (42) are more complicated than solution (49). In this case one of the two domains which are separated by the wall must be unstable and two processes should occur simultaneously. Firstly, the domain wall moves and secondly, the director in the unstable domain reorientates toward the stable equilibrium state. The second process proceeds very slowly if $B \simeq B_0$ and $\kappa^{(3)} \ll 1$, so that the wall motion can be observed for a relatively long time. A solution of equation (42) describing both processes has not yet been found. But the observation of walls [5] at fields somewhat below B_1 is explained by the slow decay rate of unstable domains.

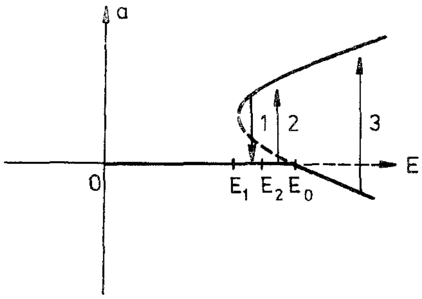

Figure 7. Bifurcation diagram of a S_C sample, which is subject to an electric field (E is the electric field and a is the distortion amplitude). The arrows indicate transitions from a metastable to an absolutely stable state by travelling domain walls.

6.2. *Smectic C film*

Recently, experimental results concerning the domain wall motion in non-chiral smectic C films has been reported [6]. The wall motion observed above the Freedericksz threshold was interpreted as a transition of a metastable distorted state to the absolutely stable director configuration, which corresponds to transition 3 in figure 7 of the present paper. The wall velocity

$$V = \frac{\lambda(B_{el}\Delta\varepsilon)\sin\kappa\cos\theta E}{\lambda}, \quad (82)$$

obtained in [6] refers to a large field strength $E \gg E_0$ and therefore differs from equation (76), which is valid in the neighbourhood of E_0.

It should be mentioned, that a transcritical bifurcation is also possible in nematic cells with a boundary pretilt angle, when an inclined magnetic field is oriented exactly perpendicular to the director [15]. In this case analogous formulas for domain walls as obtained in §5.2 result.

References

[1] De Gennes, P. G., 1974, *The Physics of Liquid Crystals* (Oxford University Press).
[2] Brochard, F., 1971, *J. Phys., Paris*, **33**, 607.
[3] Wang, X. Y., 1985, *Physics Lett.* A, **112**, 402.
[4] Lin, L., and Shu, C. Q., 1986, *Physics Lett.* A, **119**, 178.
[5] Leger, L., 1973, *Molec. Crystals liq. Crystals*, **24**, 33.
[6] Schiller, P., Pelzl, G., and Demus, D., 1987, *Liq. Crystals*, **2**, 21.
[7] Lin, L., Shu, C. Q., and Xu, G., 1985, *J. statist. Phys.*, **39**, 633.
[8] Shao, R. F., Zheng, S., Liang, Z. C., Shu, C. Q., and Lin, L., 1987, *Molec. Crystals liq. Crystals*, **144**, 345.
[9] Xu, G., Shu, C. Q., and Lin, L., (1985), *J. math. Phys.*, **26**, 1566.

[10] Xu, G., Shu, C. Q., and Lin, L., 1987, *Phys. Rev.* A, **36**, 277.
[11] Iooss, G., and Joseph, D. D., 1980, *Elementary Stability and Bifurcation Theory* (Springer-Verlag).
[12] Schiller, P., 1989, *Liq. Crystals*, **4**, 69.
[13] Ebeling, W., and Feistel, R., 1982, *Physik der Selbstorganisation und Evolution* (Akademie-Verlag).
[14] Yu-zhang, X., and Zhong-can, O. Y., 1988, *Phys. Rev.* A, **37**, 5002.
[15] Derfel, G., 1988, *Liq. Crystals*, **3**, 1411.